Supplementary Material

Table S1. Freezing level values (m a.s.l) obtained from each season. IQR range comes to the range obtained from H_0 values from meridional (IQRm) and zonal profile (IQRz). Trough the maximum and minimum the variability is represented. $\bar{H}_0$ is the temporal and spatial mean, while H_0 represent only the temporal mean in the season.

	$\bar{H}_0$	$H_0^{Max.}$	$H_0^{Min.}$	Max. ($\bar{H}_{0,m}$ + IQRm)	Min. ($\bar{H}_{0,m} - IQRm$)	Max. ($\bar{H}_{0,z} + IQRz$)	Min. ($\bar{H}_{0,z} - IQRz$)
Summer	2236	3346.2	1227.6	3383.3	1187.5	3383.3	931.3
Autunm	1891	2870	1068.3	2848.2	1065.7	2858.1	841.4
Winter	1169	1981.8	575.4	1798.8	590.7	1930.7	446.7
Spring	1477	2440	728.3	2448.5	701.1	2440.9	596.1
Annual	1691	2657.7	913.1	2625.9	904.8	2654.2	705.4

Table S2. Trends values (m/decade) obtained from each season. IQR range corresponds to the range obtained from trend values for meridional (IQRm) and zonal profile (IQRz). Trough the maximum and minimum the variability is represented.

	$T_0^{Max.}$	$T_0^{Min.}$	Max. ($\bar{T}_{0,m}$ + IQRm)	Min. ($\bar{T}_{0,m} - IQRm$)	Max. ($\bar{T}_{0,z} + IQRz$)	Min. ($\bar{T}_{0,z} - IQRz$)
Summer	60.7	18.1	58.3	18.6	68.2	18.6
Autunm	45.5	17.5	44.8	17.3	46.4	22.6
Winter	30.1	8.4	31.1	10.2	29.5	8.9
Spring	22.4	10.5	21	10.6	23.4	11.9

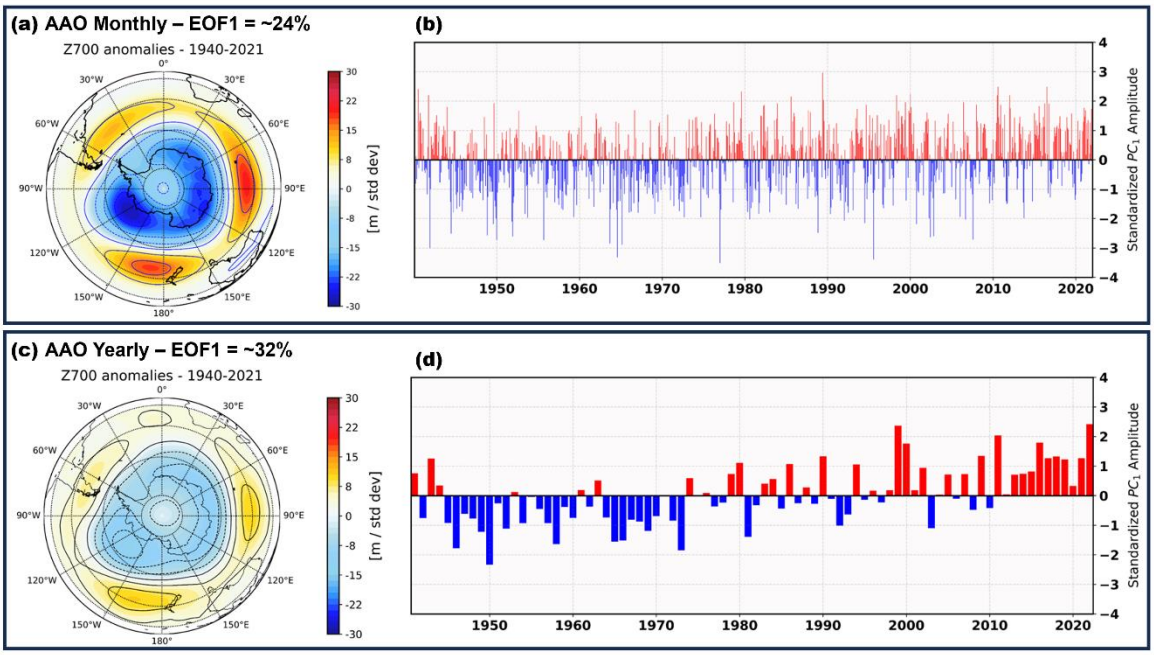

Figure S1. Leading Empirical Orthogonal Function (EOF) of ERA5 700 hPa geopotential height through two datasets: (a) monthly mean data, and (c) annual mean data spanning from 1940 to 2021. The EOFs are generated from detrended 700 hPa geopotential height anomaly data, weighted by the square root of the cosine of latitude, within the latitude range of 20° to 90°S. The resulting patterns are displayed as regression maps, depicting the interplay between the leading Principal Component (PC) time series and the spatial distribution of the evolving height anomalies (b and d, respectively). The temporal pattern is illustrated by blue and red bars (negatives/positive values) of the first Principal Component, scaled to unit variance (divided by the square root of its eigenvalue). Each panel includes insights into the proportion of explained variance and showcases the standardized PC time series grounded in the NOAA Climate Prediction Center's (CPC) 1979-2000 reference period.

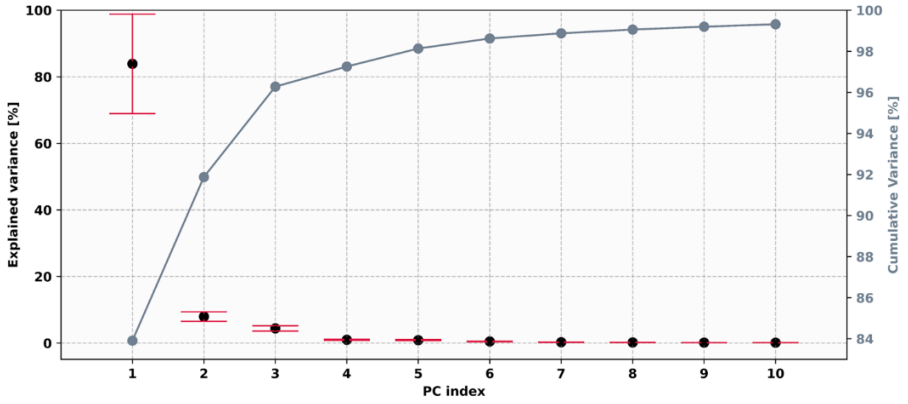

Figure S2. Eigenvalues of the top ten leading modes of variability for the annual H0 field in Patagonia, obtained through the EOF analysis (black dots), and their associated typical errors (red bars), following the method of North et al., (1982). Moreover, the accumulated percentage of the total variance explained by each principal component (gray dots) is depicted on the right axis.

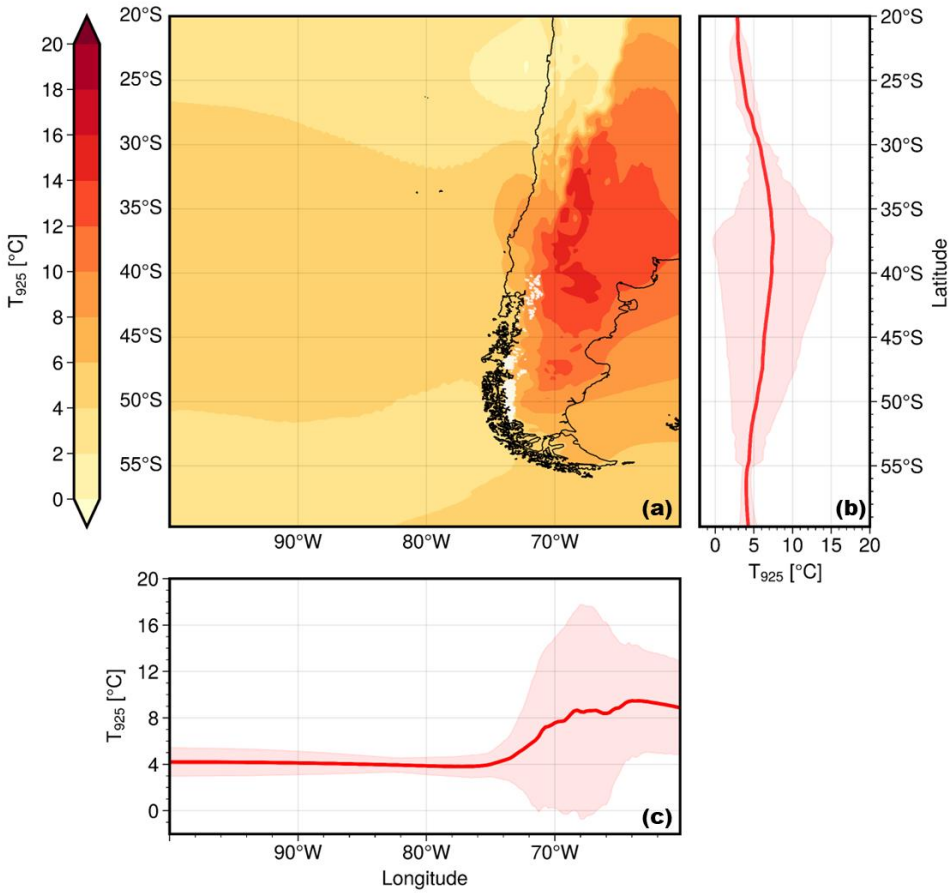

Figure S3. Spatial distribution of the January minus July mean air temperature at 925 hPa. Lighter areas depict a lower temperature, while red areas indicate higher values. The white contours delineate the extent of ice coverage in the region. Each distribution is accompanied by a latitudinal profile (b) and a longitudinal profile (c), showcasing the spatially averaged temperature values. The red shaded area in these profiles represents the interquartile range.

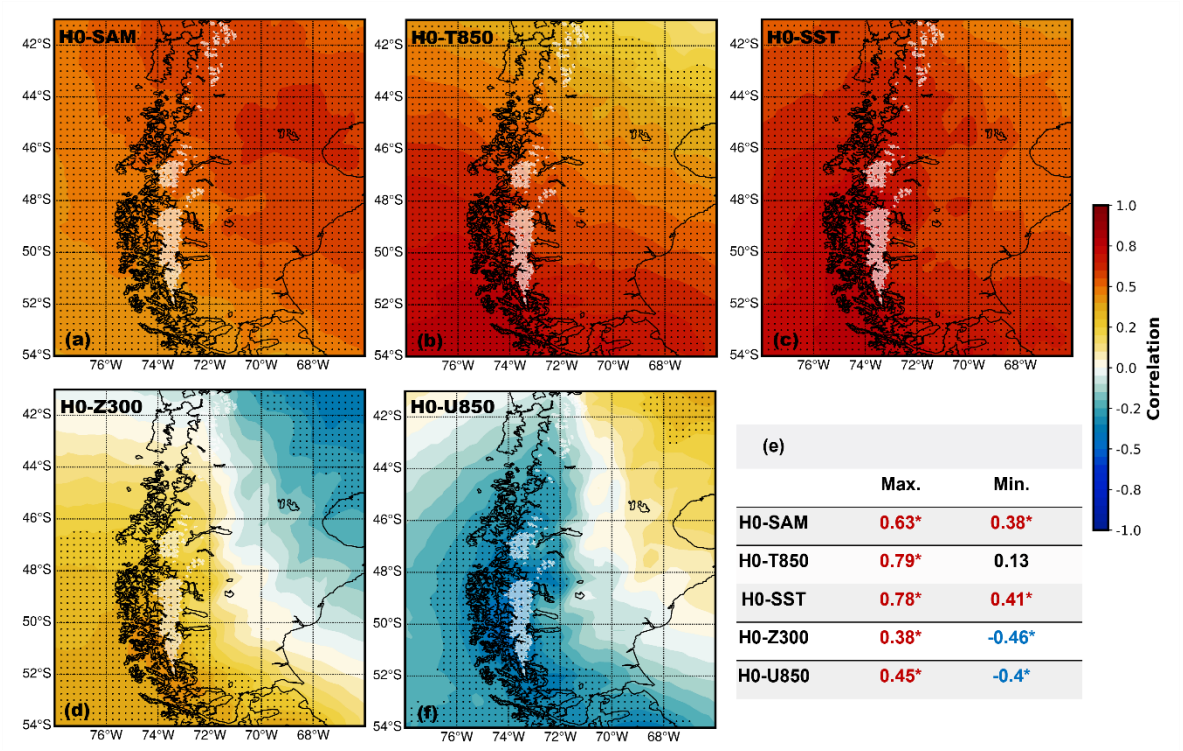

(e)

	Max.	Min.
H0-SAM	0.63*	0.38*
H0-T850	0.79*	0.13
H0-SST	0.78*	0.41*
H0-Z300	0.38*	-0.46*
H0-U850	0.45*	-0.4*

Figure S4. Spatial correlation maps between the detrended annual mean isotherm field and the detrended custom indices timeseries SAM (a), T850 (b), SST (c), Z300 (d), and U850 (f). The white contours outline the ice coverage boundaries within the region. Black circles denote statistically significant correlations. (e) Correlation chart with the maximum and minimum values of every spatial field showed, where the asterisk symbol (*) indicates statistical significance (p-value < 0.05). Red (blue) correlation values depicted positive (negative) correlations.